Evolution of Darwin's *Peloric* Gloxinia (*Sinningia speciosa*) Is Caused by a Null Mutation in a Pleiotropic TCP Gene

Yang Dong,[†,‡,1] Jing Liu,[†,1,2] Peng-Wei Li,[1,2] Chao-Qun Li,[1,2] Tian-Feng Lü,[1,2] Xia Yang,[1] and Yin-Zheng Wang*[,1,2]

[1]State Key Laboratory of Systematic and Evolutionary Botany, Institute of Botany, Chinese Academy of Sciences, Xiangshan, Beijing, China

[2]University of Chinese Academy of Sciences, Beijing, China

[†]These authors contributed equally to this work.

[‡]Present address: Department of Crop Genetics, John Innes Centre, Norwich Research Park, Norwich, UK

***Corresponding author:** E-mail: wangyz@ibcas.ac.cn.

Associate editor: Michael Purugganan

The full length of *SsCYC* and *Sscyc* genomic DNA have been deposit into NCBI under the accession number MG674379 and MG674380, respectively. The sequence matrix used in the study have been deposit into TREEBASE (study 22553, http://purl.org/phylo/treebase/phylows/study/TB2: S22553, last accessed April 11, 2018).

Abstract

Unlike most crops, which were domesticated through long periods of selection by ancient humans, horticultural plants were primarily domesticated through intentional selection over short time periods. The molecular mechanisms underlying the origin and spread of novel traits in the domestication process have remained largely unexplored in horticultural plants. Gloxinia (*Sinningia speciosa*), whose attractive *peloric* flowers influenced the thoughts of Darwin, have been cultivated since the early 19th century, but its origin and genetic basis are currently unknown. By employing multiple experimental approaches including genetic analysis, genotype–phenotype associations, gene expression analysis, and functional interrogations, we showed that a single gene encoding a TCP protein, *Ss*CYC, controls both floral orientation and zygomorphy in gloxinia. We revealed that a causal mutation responsible for the development of *peloric* gloxinia lies in a 10-bp deletion in the coding sequence of *SsCYC*. By combining genetic inference and literature searches, we have traced the putative ancestor and reconstructed the domestication path of the *peloric* gloxinia, in which a 10-bp deletion in *SsCYC* under selection triggered its evolution from the wild progenitor. The results presented here suggest that a simple genetic change in a pleiotropic gene can promote the elaboration of floral organs under intensive selection pressure.

***Key words:* peloric gloxinia, *Sinningia speciosa*, domestication, molecular mechanism, floral horizontal orientation, pleiotropic gene.**

Article

Introduction

The interaction between humans and plants is best characterized by horticultural domestication, which is intimately associated with the development of modern civilization over the last 300 years (Janick 2005; Kingsbury 2009). Horticultural plants were domesticated by humans through intentional selection, usually by crossing different varieties to alter morphological characters for ornamental, medicinal or religious purposes, over a relatively short time period (Doebley et al. 2006; Kingsbury 2009). Some horticultural plants, like *Petunia* and *Primula*, were wildly used as model system to develop genetic toolkits for experimental studies in evolution of floral traits and speciation under natural selection regime (Hoballah et al. 2007; Amrad et al. 2016; Li et al. 2016; Sheehan et al. 2016). However, the origin of horticultural characters arising from domestication have remained practically unexplored in most horticultural plants at the molecular level.

Gloxinia is a tropical gesneriacious plant native to Brazil and was domesticated in Great Britain in the early 19th century for its large attractive *peloric* flowers. The *peloric* gloxinia was originally documented in 1845, and famously became known as Darwin's *peloric* gloxinia. Distinct from the *peloric* variety, the wild progenitors produce nodding zygomorphic flowers that is adapted to insect pollination (fig. 1) (Loddiges 1817; Harrison 1847; Darwin 1868). The genetic control of floral zygomorphy was best characterized in the model species *Antirrhinum majus* with isolation and function investigation of two paralogous TCP (*TEOSINTE BRANCHED1*, *CYCLOIDEA*, and *PCF*) genes *CYCLOIDEA* (*CYC*) and *DICHOTOMA* (*DICH*) (Luo et al. 1996, 1999). *CYC* and *DICH* establish zygomorphic floral patterning by specifying the dorsal organ identities in the second and third whorls (Luo et al. 1996, 1999). In the Gesneriaceae, the *CYC*-like genes were demonstrated to be involved in the development of zygomorphic flowers, with diverse morphological variation (Song et al. 2009; Yang et al. 2012, 2015). Previously, Citerne et al. (2000) isolated a partial coding

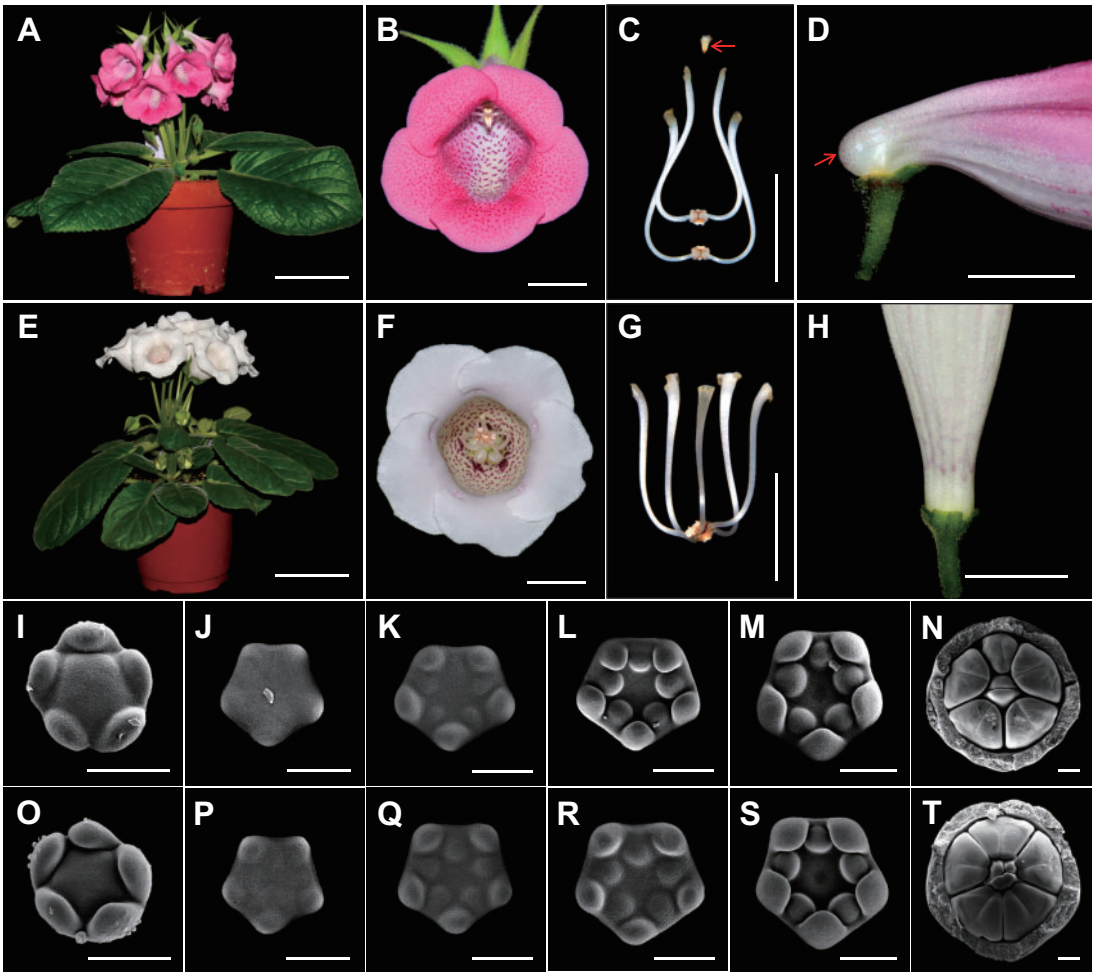

FIG. 1. Phenotypic analysis of flower character development in the wild-type and cultivated *peloric* gloxinia. (*A*) Plant architecture of wild-type gloxinia (WT-PF), showing the horizontally oriented zygomorphic flower. (*B*) Front view of WT-PF flower. (*C*) Stamen of WT-PF, the red arrow denotes the dorsal staminode. (*D*) Side view of WT-PF floral tube (sepals are removed), showing the gibbous structure (arrow). (*E*) Plant architecture of cultivated *peloric* gloxinia (MU-WB), showing the upright actinomorphic flower. (*F*) Front view of MU-WB flower. (*G*) Stamen of MU-WB. (*H*) Side view of MU-WB floral tube (sepals are removed), showing the loss of the gibbous structure. (*I*–*N*) Floral developmental series of wild-type gloxinia (WT-PF) revealed by SEM. (*I*) The sepals initiated and developed equally. (*J*) The petal primordia arise subsequently inside the five sepals (removed). (*K*) The stamen primordia emerge inside the five petals in an alternating pattern. (*L*–*N*) As the floral organs advance in development, the floral zygomorphy manifests with the two dorsal petals slightly smaller than the lateral and ventral ones (*L* and *M*), and the dorsal stamen is finally suppressed into a staminode in development (*N*). (*O*–*T*) Floral developmental series of *peloric* gloxinia (MU-WB) revealed by SEM. (*O*) The sepals initiated and developed equally. (*P*) Petal primordia emerge subsequently inside the five sepals (removed). (*Q*) The stamen primordia arise inside the five petals in an alternative pattern. (*R*, *S*) As the development program proceeds, all the floral organs in each whorl develop equally. (*T*) The five stamens are equally differentiated into fertile stamens. Scale bar in (*A*, *E*), 10cm; (*B*–*D* and *F*–*H*), 1cm; (*I*–*T*), 100μm.

sequence of *GCYC* from a *peloric* gloxinia cultivar and observed a single adenine base deletion immediately downstream of the TCP domain. It was therefore proposed that the deletion and resulting truncated protein promotes the development of the *peloric* phenotype (Citerne et al. 2000). However, subsequent resequencing of *GCYC* from other *peloric* gloxinia accessions showed that the adenine deletion is probably a PCR artefact (Zaitlin 2011; also see Smith et al. 2004), implying that the molecular mechanism underlying the *peloric* gloxinia is more complicated than previously hypothesized.

It has long been recognized that floral orientation is intimately associated with floral symmetry (Sprengel 1793; Robertson 1888; Darwin 1865). However, the floral orientation has received little attention to date, despite the fact that floral symmetry and the evolution of zygomorphy is an important trend in angiosperm radiation (Dilcher 2000; Preston and Hileman 2009; Hileman 2014a). The floral horizontal orientation has evolved as an adaption to enable efficient pollination, likely representing the first step towards floral specialization (Fenster et al. 2009; Wang et al. 2014). In fact, the floral horizontal orientation and zygomorphy usually covary in angiosperms, particularly in sympetalous groups (supplementary table S1, Supplementary Material online). Deciphering whether these highly linked traits are underpinned by multiple factors or simple genetics would promote an understanding of the complex mechanisms behind floral evolution in angiosperms.

In this study, we explore the molecular mechanisms underlying the evolution of the *peloric* characteristics of cultivated gloxinias, and further determine its origin by employing a highly combinatorial experimental approach. We have characterized a 10-bp deletion in the coding sequence of TCP-coding gene *Sscyc* that likely results in the production of a nonfunctional truncated protein with 45 amino acid (aa) in length. We demonstrate that this mutation is causally responsible for the development of *peloric* flowers in gloxinia. The putative ancestor of modern *peloric* gloxinias was further traced back to a particular wild collection from Rio de Janeiro State in 1820 (*G. caulescens*, now a synonym of *S. speciosa*) by literature review, and genetic inference combined with phylogenetic analysis. The results show that one mutation in a single gene causes a complex morphological shift from a horizontally orientated, and zygomorphic flower, to an upright, actinomorphic form in gloxinia. Our findings suggest that pleiotropy may play a crucial role in the coordinated evolution of complex floral organs in angiosperms.

Results

Phenotypic and Genetic Analysis of the *Peloric* Character in Gloxinia

Wild-type gloxinia flowers are zygomorphic (bilaterally symmetric) and horizontally orientated (fig. 1*A*). The floral zygomorphy is weak in the second whorl, where the dorsal petals are only slightly smaller than the lateral and ventral ones, and strong in the third whorl, where the dorsal stamen is present as a staminode (fig. 1*A–C* and supplementary fig. S1, Supplementary Material online). The horizontal orientation of the flower is caused by a ventral–dorsal asymmetric growth at the base of dorsal corolla which produces a convex, gibbous structure (fig. 1*D*). Meanwhile, the *peloric* flowers are actinomorphic (radially symmetric) and upright without the development of a gibbous structure (fig. 1*E–H* and supplementary fig. S1, Supplementary Material online). In order to determine whether these two floral traits are tightly correlated in a broad range of taxonomic groups, we conducted a morphological survey covering all families of sympetalous angiosperms, and found that the horizontal placement of the floral tube is largely associated with the zygomorphic state of flowers (supplementary table S1, Supplementary Material online). This result suggests that the combination of these morphological traits conferred a selective advantage during floral evolution in angiosperms.

To determine the genetics of the *peloric* phenotype, we crossed the wild-type zygomorphic gloxinia "Pink Flower" (WT-PF) with *peloric* gloxinia "White Bell" (MU-WB) (Materials and Methods). All 13 F_1 plants exhibited a WT phenotype with a typical horizontally orientated zygomorphic flower (fig. 2*A*), implying that the *peloric* phenotype is recessive. Representatives of F_1 plants were selfed to produce an F_2 segregating population with a 3:1 ratio of WT to *peloric* phenotypes (141: 41; $\chi^2 = 0.593$, $f = 1$, $P = 0.441$) (fig. 2*A*), suggesting that *peloria* in gloxinia is a Mendelian character. We observed a perfect association (100%) between the floral zygomorphy and a horizontally orientated floral tube in the F_2 segregating population (fig. 2*A*), indicating that the *peloric* phenotype, that is, floral actinomorphy and standing upright, is controlled by recessive mutation(s) in a single gene, or closely linked genes.

Expression of *SsCYC* Is Correlated with the Development of Horizontally Orientated Zygomorphic Flowers

CYCLOIDEA (*CYC*)-like TCP genes are known to be involved in the genetic control of floral zygomorphy in a broad array of species (Luo et al. 1996; see review in Preston and Hileman 2009). In Gesneriaceae, an ancient gene duplication event occurred prior to the split of the Gesnerioideae and the Cyrtandroideae subfamilies generating *GCYC1* and *GCYC2* paralogous lineages (Citerne et al. 2000; Smith et al. 2004). We cloned the full length *Sinningia speciosa CYC* (*SsCYC*) gene, and performed a phylogenetic analysis. The results indicate that the Gesnerioideae subfamily, which includes the *Sinningia* genus, has lost the *GCYC1* lineage in evolution and harbours only one copy of the *CYC*-like genes, belonging to the *GCYC2* clade, which is homologous to *AmCYC*/*AmDICH* (supplementary fig. S2, Supplementary Material online).

Ontogenetic analysis shows that the floral organ development of WT-PF and MU-WB exhibits a similar pattern before the stamen initiation with all primordium developed equally (fig. 1*I–K* and 1*O–Q*). Later on, the developmental differences between them become evident in the dorsal floral organs with their growth suppressed in WT-PF (fig. 1*L–N* and 1*R–T*). Correlatively, *SsCYC* shows a weak dorsal specific expression pattern in the petal whorl, and strong asymmetric expression in the stamen whorl, with an extremely high level of expression in the staminode in WT-PF (fig. 3*B*, *C*, and *G*). In contrast, all floral organs develop equally in MU-WB, and no *Sscyc* expression can be detected during petal and stamen development (figs. 1*O–T* and 3*E* and *H*). In the floral tube of WT-PF, the expression of *SsCYC* seems to be exceptionally high in the gibbous structure compared with other sampled tissues, whereas its expression in the Dorsal Floral Tube (DFT) is only slightly higher relative to those in the Ventral Counterparts of the gibbous structure (VC) and the Ventral Floral Tube (VFT) (fig. 4*I* and *J*). In MU-WB, only a residual *Sscyc* expression signal can be detected in the sampled tissues of the floral tube (fig. 4*J*). The RNA in situ hybridization shows that the *SsCYC* expression exhibits an asymmetric gradient pattern in the developing gibbous structure, in which strong signals are observed in the inner cell layers whilst almost no expression can be detected in the outer cell layers (fig. 4*A*, *B*, *D*, and *F*). In contrast, no expression signal of *SsCYC* can be detected in all ventral counterparts of the gibbous structure (fig. 4*C*, *E*, and *G*). Concomitantly, the cell growth in the inner part of the gibbous structure is significantly suppressed while the cells in the outer layers and the ventral counterparts are expanded almost equally (fig. 4*K–R* and supplementary fig. S3, Supplementary Material online). As outlined above, the specific expression of *SsCYC* is correlated with a suppression of growth in the dorsal floral organs, and a suppression of cell expansion in the inner part of the gibbous structure.

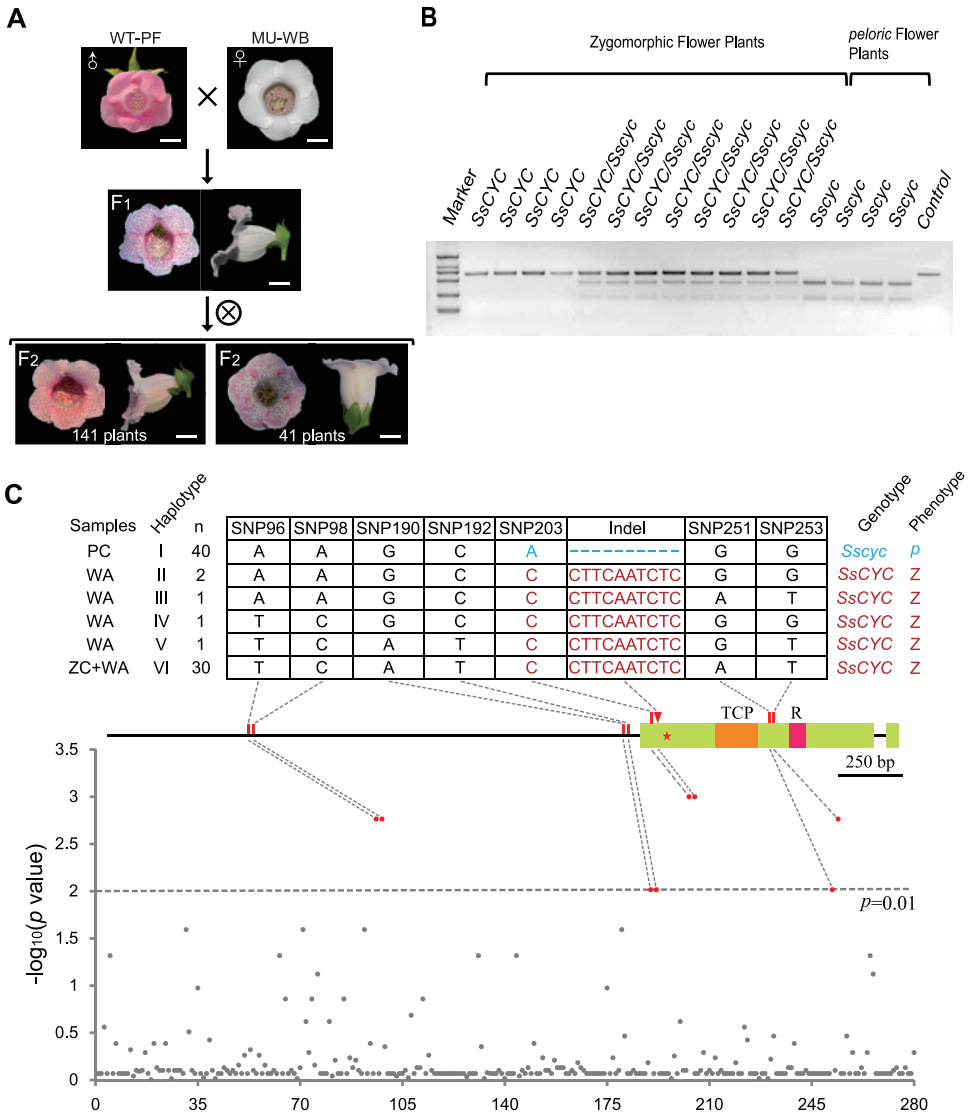

Fig. 2. Genetic and association analysis of *peloric* flower in gloxinia. (*A*) Representatives of F_1 and F_2 plants of WT-PF × MU-WB. (*B*) Genotyping of F_2 plants by CAPS. 16 representatives of F_2 progenies are shown in the gel. Control experiment (Control) was conducted with *SsCYC* homozygous PCR product with no *Nde* I treatment. (*C*) Genotype–phenotype association analysis with variation sites in the 3,111-bp sequence of the *SsCYC* locus. In the upper panel, haplotypes of the significantly associated variation sites with *n* denote the number of sequences that are included in each haplotype; the variation sites that have consistent association between genotype and phenotype are colored in blue and red, respectively. The middle panel illustrates the gene structure of *SsCYC*. The TCP domain and R domain are shaded in orange and pink, respectively. The significant associated SNPs and Indel are indicated by red bars and triangles, respectively. In the bottom panel, grey circles represent variation sites that are not significantly associated with the *peloric* flower character, whilst the red circles represent SNPs or Indel significantly associated with the *peloric* flower character. PC, *Peloric* Cultivars; WA, Wild Accessions; ZC, Zygomorphic-flowered Cultivars; *p*, *peloric* flower; Z, zygomorphic flower. Scale bar in (*A*), 1cm.

The *Peloric* Phenotype Is Associated with a 10-bp Deletion in the Coding Sequence of *Sscyc*

To determine whether the *peloric* mutation maps to the *SsCYC* locus, we genotyped 182 F_2 plants of WT-PF × MU-WB using Cleaved Amplified Polymorphic Sequences (CAPS). The *SsCYC* allele (wild-type) perfectly cosegregated with the phenotype of horizontally orientated zygomorphic flowers, and all upright *peloric* flowers were homozygous for the mutant *Sscyc* allele (fig. 2*B*). In addition, we also genotyped 36 modern accessions of gloxinia with either zygomorphic or *peloric* phenotype from various geographic locations around the globe. This result confirmed the genotype–phenotype correlation revealed from the analysis of the F_2 population (supplementary table S2 and fig. S4, Supplementary Material online).

A careful comparison of the 3,111-bp genomic DNA sequences (including 1992-bp 5′ promoter sequence) between WT-PF and MU-WB revealed 56 SNPs and one Indel (data not shown), but failed to resolve the causal mutation for *peloria*. In order to find the causal mutation, we took a SNP-phenotype association analysis using a panel of 75 gloxinia accessions (52 cultivated accessions and 23 wild

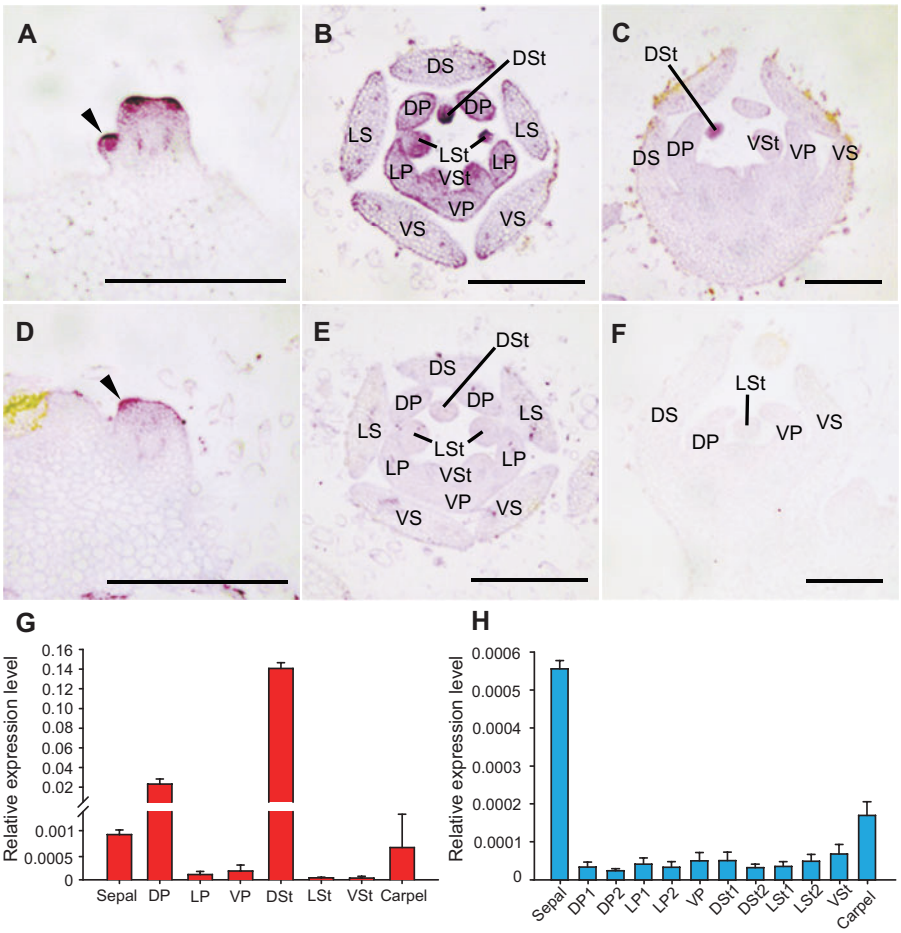

Fig. 3. Comparative expression analysis of *SsCYC*/*Sscyc* in WT-PF and MU-WB. (*A*) The *SsCYC* mRNA can be detected across the apex of the young floral meristems of WT-PF (triangle). (*B*) In WT-PF, *SsCYC* is evenly distributed in the petal and stamen primordia with an extremely high level detected in dorsal staminode. (*C*) As the developmental program proceeds, the *SsCYC* mRNA is specifically accumulated in the dorsal stamens and is undetectable in the other floral organs of WT-PF. (*D*) *Sscyc* mRNA is evenly distributed in the young floral meristems of MU-WB. (*E*) Its transcripts can no longer be detected in the subsequent development stages of MU-WB. (*F*) Control experiment with sense *SsCYC* probe generated no signal in WT-PF flower of stage similar to (*C*). (*G*) Expression analysis of *SsCYC* in WT-PF floral organs. (*H*) Expression analysis of *Sscyc* in MU-WB floral organs. DS/LS/VS, Dorsal/Lateral/Ventral Sepals; DP/LP/VP, Dorsal/Lateral/Ventral Petals; DSt/LSt/VSt, Dorsal/Lateral/Ventral Stamen; DFT/VFT, Dorsal/Ventra Floral Tube; GS, Gibbous Structure; VC, Ventral Counterpart of the GS. FD, Floral Discs; Error bars in (*G* and *H*) indicate S.D. of three biological replicates. Scale bars in (*A*–*F*), 100 μm.

collections) collected from different geographic regions (supplementary table S2, Supplementary Material online). We identified a total of 29 distinct haplotypes in that seven SNPs and one Indel were significantly associated with the *peloric* phenotype ($P < 0.01$) (fig. 2C and supplementary table S3, Supplementary Material online). Further analysis of these sites within six haplotypes showed that four SNPs in the regulatory region (SNP96, SNP98, SNP190, and SNP192) and two in the coding region (SNP251 and SNP253) are completely or partially shared between *peloric* cultivars and three or more zygomorphic accessions, thus excluding them from having a functional relevance to the *Sscyc* allele (fig. 2C). Of the remaining two sites, SNP203 (A/C, +46 bp) is unlikely to be responsible for *peloria*, as the amino acid substitution (Serine/Tyrosine) lies outside of the TCP domain, and therefore is unlikely to alter the activity of SsCYC. The Indel (-CTTCAATCTC, +48 bp) causes a frameshift in the coding sequence, which results in a truncated protein with 45-amino acids in length. This truncated protein is likely nonfunctional as it lacks the entire TCP domain and the downstream C terminus (fig. 2C).

Functional Analyses of *SsCYC*/*Sscyc* Confirm Its Role in *Peloric* Gloxinia Development

To validate the biological function of *SsCYC* and *Sscyc*, we fused the coding sequences of the alleles with the CaMV 35S promoter and transformed *Arabidopsis thaliana*. T1 transgenic plants were selfed to produce T2 populations (see methods). The heritability of the transgene was confirmed by RT-PCR (supplementary fig. S5, Supplementary Material online). Compared with WT plants, the *SsCYC* overexpression lines showed retarded plant development (fig. 5A) with smaller leaves (supplementary figs. S6 and S8, Supplementary Material online) and smaller floral organs (supplementary figs. S7 and S8, Supplementary Material online). Meanwhile,

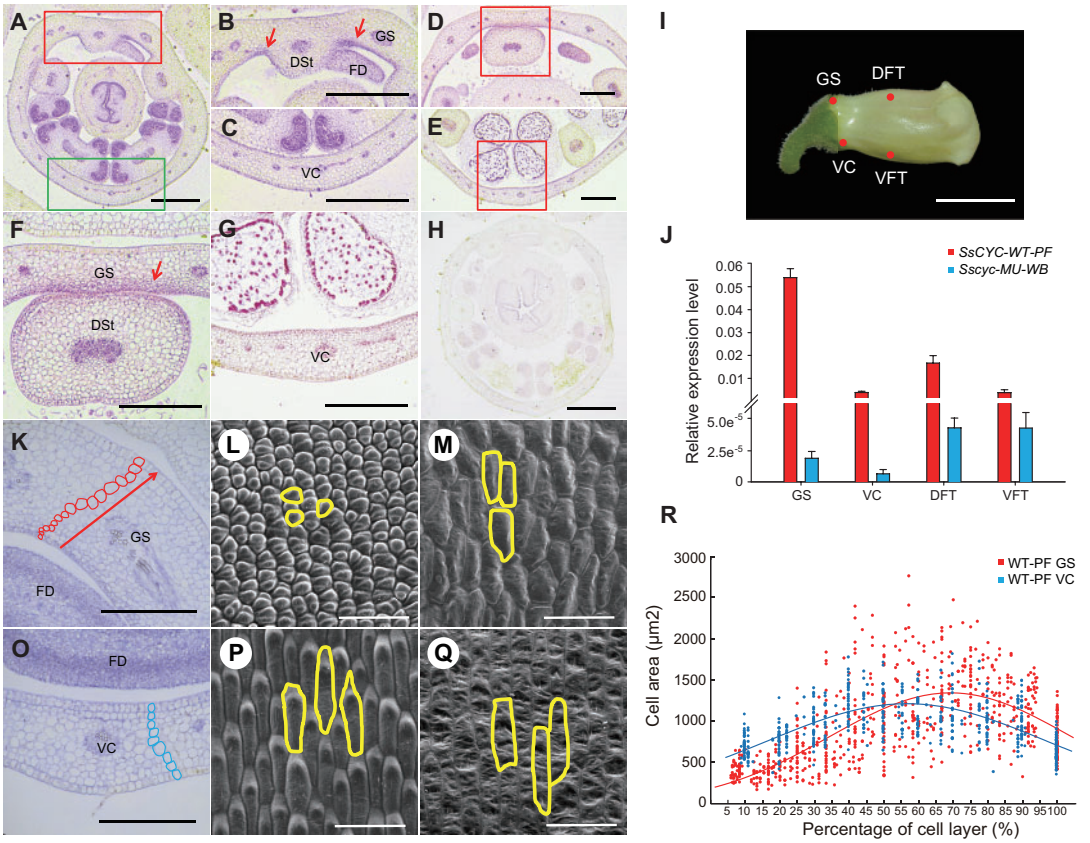

Fig. 4. Gene expression and cell morphology analysis of the gibbous structure in WT-PF. (*A*–*H*) *SsCYC* expression analysis in the developing GS and floral tube of WT-PF. (*A*) *SsCYC* signals are specifically localized in the inner cell layer (red arrows) of GS but not in the VC (enlarged in *B* and *C*, respectively). (*D* and *E*) In late floral developmental stages when the anthers were differentiated, *SsCYC* expression can still be detected in the inner cell layers (red arrow) of the GS (*D*, enlarged in *F*), but not in the VC (*E*, enlarged in *G*). (*H*) Control experiment using sense *SsCYC* probe generates no signals. (*I*) Graphic view of the floral tissues sampled for expression analysis in (*J*). (*K*) Cross sections of the GS. A single cell layer is marked in red to show the cell size variation tendency from the inner epidermis to the outer epidermis (red arrow). (*L* and *M*) SEM analysis of the epidermal cells of WT-PF GS showing that cell expansion is extremely suppressed in the inner epidermis (*L*) compared with the outer epidermis (*M*). (*O*) Cross sections of the VC. A single cell layer is marked in blue to show no obvious variation of cell size from the inner epidermis to the outer epidermis. (*P* and *Q*) SEM analysis of the epidermal cells of ventral counterparts of gibbous structure showing that no cell expansion difference can be detected. (*R*) Scatterplot of cell size (μm^2) and relative position of the cell from the inner epidermis (0%) to the outer epidermis (100%). Gaussian Fitting was calculated to show the variation tendency of cell size along the dorso-ventral axis of the tissue. GS, gibbous structure; VC, Ventral Counterpart of the GS; FD, Floral Disc. Scale bar in (*A*–*H*), 150 μm; (*K* and *O*), 100 μm; (*L*, *M*, *P*, and *Q*), 50 μm; (*I*), 0.5 cm.

Sscyc overexpression generated no obvious phenotypic changes (fig. 5*A* and supplementary figs. S6–S8, Supplementary Material online). Further SEM analysis of the epidermis of leaves and petals showed that cell expansion was repressed in *SsCYC* overexpression lines (fig. 5*B* and *C* and supplementary fig. S6, Supplementary Material online), which is consistent with our hypothesis that dorsal-specific expression of *SsCYC* suppresses the growth of the dorsal floral organs (figs. 1*A*–*C* and 4*K*–*M*). In contrast, no evident changes were observed regarding the cell morphologies in leaves or petals in *Sscyc* overexpressing lines, indicating that Sscyc protein is nonfunctional (fig. 5*B* and *D* and supplementary figs. S6 and S8, Supplementary Material online). Therefore, the development of the *peloric* gloxinia may be attributed to the 10-bp deletion in *Sscyc* and the resultant truncated non-functional protein.

Chimeric Repressor Silencing Technology (CRES-T) was recently developed as a powerful tool to knock-down endogenous genes by converting transcriptional activators into strong repressors when the target gene is fused to the ERF-associated Amphiphilic Repression (EAR) motif (SRDX, Hiratsu et al. 2003). Considering that *SsCYC* is the only copy of the *CYC*-like gene in the gloxinia genome (supplementary fig. S2, Supplementary Material online), we next tried to repress *SsCYC* function by producing transgenic plants with 35S: SsCYC: SRDX in WT-PF gloxinias (Materials and Methods) (supplementary fig. S9, Supplementary Material online). The plants regenerated from untransformed leaf cultures produce flowers with the typical WT zygomorphic appearance with nodding floral tubes (fig. 5*E*–*G*). Among ten independent transgenic plants expressing the 35S: SsCYC: SRDX fusion protein, three developed upright actinomorphic flowers with fully ventralized petals and stamens, perfectly phenocopying the flowers of *peloric* gloxinias (fig. 5*H*–*J*). In addition, we did not observe any phenotypic alterations in these transgenic plants other than floral symmetry changes, suggesting the SsCYC: SRDX fusion

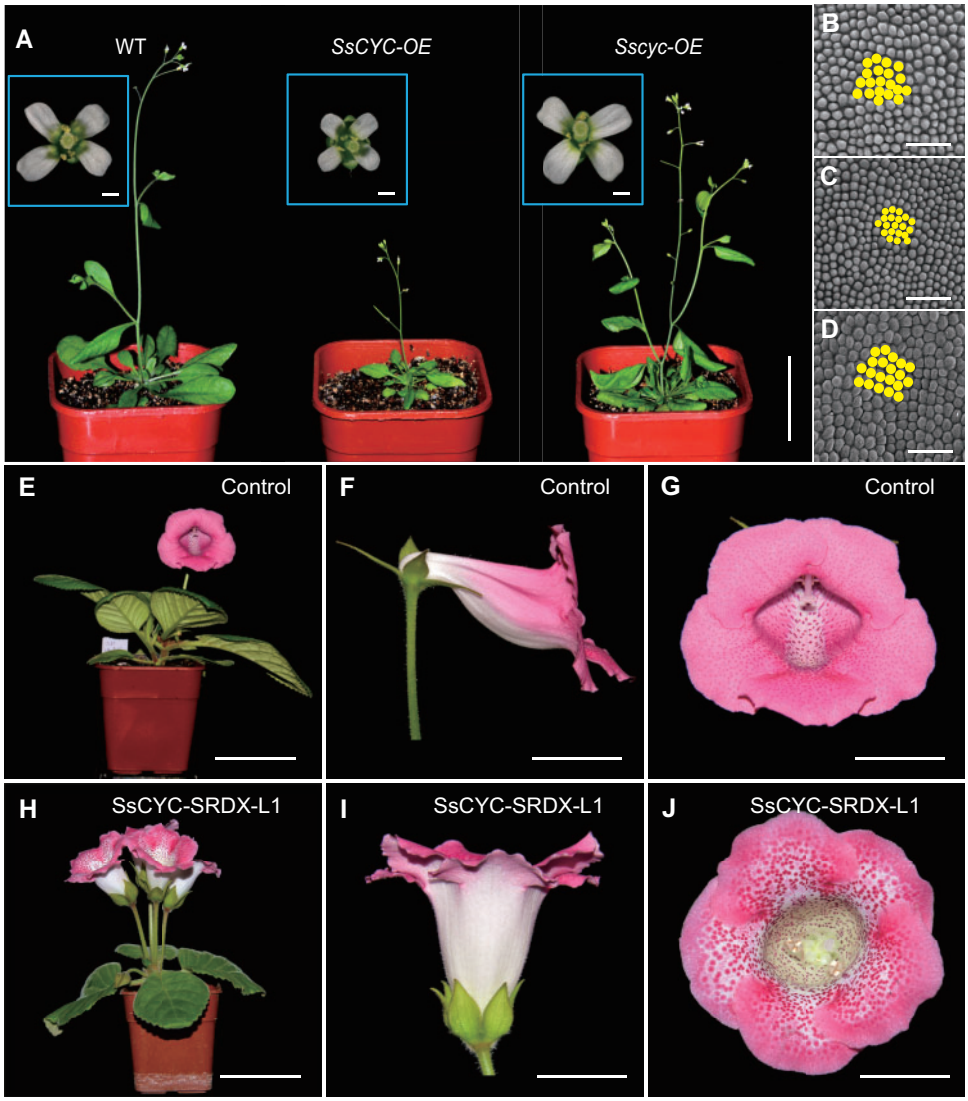

Fig. 5. Functional analysis of *SsCYC*/*Sscyc* in *Arabidopsis* and CRES-T analysis of *SsCYC* in WT-PF. (*A*) Overexpression of *SsCYC* in *Arabidopsis* retards plant development while overexpression of *Sscyc* in *Arabidopsis* generates no phenotypic alteration. The inserts show the flowers of each genotype. SEM analysis of the petal epidermal cells of WT plants (*B*), *SsCYC* overexpressor (*C*) and *Sscyc* overexpressor (*D*). In (*B*–*D*), a total of 20 epidermal cells are shaded in yellow to indicate the cell size difference. (*E*) Plant architecture of the transgenic control plants. (*F*) Side view of the horizontally oriented flower character of the transgenic control plants. (*G*) Front view of the wild-type zygomorphic flower of the transgenic control plants. (*H*) Plant architecture of the SsCYC-SRDX transgenic plants (SsCYC-SRDX-L1), showing the upright *peloric* flowers. (*I*) Side view of the upright *peloric* flower from the SsCYC-SRDX transgenic plants (SsCYC-SRDX-L1). (*J*) Front view of the *peloric* flower from the SsCYC-SRDX transgenic plants (SsCYC-SRDX-L1). Scale bar in (*A*), 5 cm; inserted graphs in (*A*), 1 mm; (*B*–*D*), 150 μm; (*E*, *H*), 7 cm; (*F*, *G*, *I*, *J*), 1 cm.

protein specifically targets the SsCYC pathway in the flowers (Compare fig. 5*E* and *H*). The results of functional knock-down of SsCYC by CRES-T also indicate that the *GCYC2* member of Gesnerioideae exerts similar function as the *GCYC1* members of Cyrtandroideae in repressing cell expansion in the dorsal floral organs (Yang et al. 2012; Liu et al. 2014).

Taken together, these findings indicate that a single pleiotropic gene, *SsCYC*, controls both the floral orientation and floral symmetry through its activity in the basal floral tube, petals and stamens. A 10-bp deletion in the coding sequence of *Sscyc* results in the production of a nonfunctional truncated protein, and is causally responsible for the development of *peloric* flowers in the gloxinia.

Development of *Peloric* Gloxinia Involves a Two-Fold Molecular Mechanism

Our previous study shows that the persistent dorsal specific expression of *CYC*-like gene depends on the activity of an auto-regulatory loop of *CYC*-like genes (Yang et al. 2012). Therefore, both the functional CYC protein and CYC binding sites (CBS) in the promoter are indispensable for the establishment of floral zygomorphy (Yang et al. 2012). For instance, in *Antirrhinum majus*, the loss-of-function change in amino acid coding region in the *cyc-608* mutant produces partially ventralized *peloric* flowers (Luo et al. 1996). In addition, the lack of a CBS in the promoter sequence in *Arabidopsis thaliana* leads to transient expression of *AtTCP1* in the dorsal floral primordium in the early stages, thereby producing

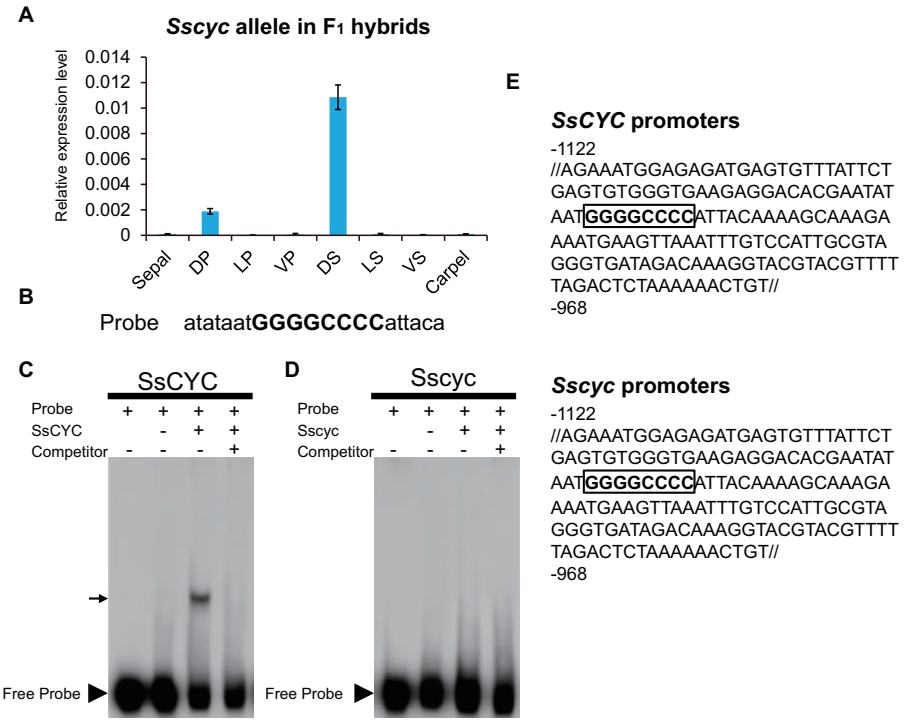

Fig. 6. Allele specific expression of *Sscyc* in F_1 hybrids and in vitro DNA–Protein interaction by EMSA. (*A*) Expression analysis of the *peloric Sscyc* allele in floral organs of the F_1 hybrid of WT-PF×MU-WB by allele-specific real-time qPCR, showing that the dorsal specific expression pattern of *Sscyc* was restored. (*B*) Oligonucleotide probe sequence used for EMSA analysis, the putative CYC-Binding Site (CBS) sequence is shown in bold capital letters. (*C*) EMSA analysis of the CBS and SsCYC recombinant protein shows that the interaction of SsCYC with CBS results in a retarded band in the gel (arrow, lane 3); the interaction of the SsCYC with CBS is abolished when excessive amounts of unlabeled probe is added (lane 4). (*D*) EMSA analysis of the CBS and Sscyc recombinant protein shows that the Sscyc protein has lost its ability to interact with the CBS sequence. (*E*) The promoter sequences of *SsCYC* and *Sscyc*. Both contain the same sequence matching the consensus CYC-Binding Sites (CBS) (boxed)

actinomorphic flowers (Cubas et al. 2001). Curiously, in the F_1 plants of WT-PF × MU-WB, we observed the restoration of dorsal specific expression of *Sscyc* by allele-specific expression analysis (fig. 6*A*). Given that initiation of *Sscyc* expression is normal in the *peloric* floral meristems as in wild-type (fig. 3*A* and *D*) and the dorsal specific expression is subsequently lost during floral organ development in the *peloric* flowers (fig. 3*B* and *E*), we hypothesized that the loss of dorsal specific expression of *Sscyc* in the *peloric* flowers resulted from the disruption of the auto-regulatory loop by the nonfunctional Sscyc protein (Yang et al. 2012). To test this idea, we compared the ~2.0 kb promoter sequence between *SsCYC* and *Sscyc*, and found that the putative SsCYC interacting element (CYC-binding Site, CBS) is conserved between WT-PF and MU-WB, that is, they share the same CBS sequence (GGGGCCC) (fig. 6*E*). Furthermore, an Electrophoresis Mobility Shift Assay (EMSA) analysis showed that SsCYC could interact with a probe containing the CBS, this binding could be effectively competed by adding excessive amounts of unlabeled CBS-containing DNA probes (fig. 6*B* and *C*). In sharp contrast, the mutated Sscyc protein failed to bind to this CBS-containing DNA sequence (fig. 6*D*).

Under both artificial and natural selection regimes, adaptive morphological traits can be produced by either change in protein function (Li et al. 2006; Hoballah et al. 2007; Pourkheirandish et al. 2015) or regulatory modifications (Chan et al. 2010; Studer et al. 2011; Dong et al. 2014). The observations presented here strongly suggest that the evolution of the *peloric* gloxinia involves a 2-fold mechanism. That is, the 10-bp deletion brings about the loss-of-function of Sscyc protein, which in turn, further disrupts the auto-regulatory loop of *Sscyc* leading to a complete loss of dorsal specific expression.

SsCYC Was Targeted by Artificial Selection during the Domestication Process of *Peloric* Gloxinia

For crops, domestication occurs when a single favoured haplotype associated with favorable morphological evolution is targeted by selection and fixed over time (Gross and Olsen 2010). To evaluate the impact of artificial selection on the *SsCYC* locus, we analyzed the DNA polymorphisms in a ~3.1 kb genomic region of *SsCYC* in a panel of 40 *peloric* accessions from diverse geographic locations, and 23 wild collections with zygomorphic flowers from Brazil (supplementary table S2, Supplementary Material online). In the wild gloxinia population, the average nucleotide diversity of *SsCYC* DNA sequence is $\pi = 0.0164$, indicative of considerable sequence polymorphism at the *SsCYC* locus (supplementary fig. S10, Supplementary Material online). However, all 40 *peloric* accessions share the same haplotype ($\pi = 0$) including the fixed 10-bp deletion in the ~3.1 kb *SsCYC* genomic sequence (supplementary fig. S10, Supplementary Material online), indicating that intensive artificial selection has targeted

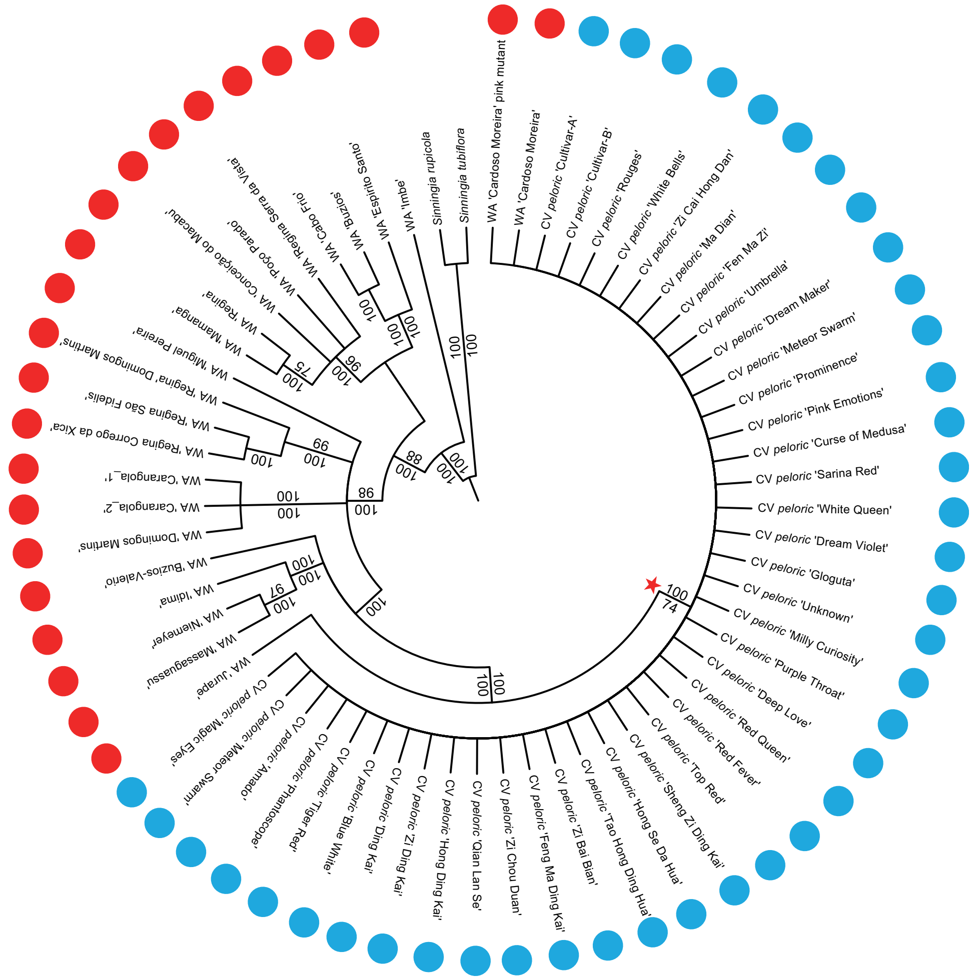

Fig. 7. Phylogenetic analysis of the *SsCYC* locus in *Sinningia speciosa*. Majority rule consensus tree of 235 most parsimonious trees generated from *SsCYC* sequences of *S. speciosa*. Bootstrap (BS) values and Bayesian Posterior Probabilities (PP) are indicated above and below the branches, respectively. The cultivated *peloric* gloxinia accessions (Cultivated, CV) and wild gloxinia accessions (Wild Accession, WA) are indicated by blue and red dots, respectively. The red star indicates the close relationship of the *peloric* gloxinia accessions with two wild gloxinia collections (*S. speciosa* "Cardoso Moreira pink mutant" and *S. speciosa* "Cardoso Moreira").

this mutation by removing rare sequence variants in this locus. To trace the origin of *peloric* gloxinias, we constructed the *SsCYC* phylogeny based on the ~1,250-bp genomic sequence. All 40 *peloric* gloxinias are grouped together with two wild gloxinias "Cardoso Moreira" in a single well supported clade (fig. 7). In contrast, the tree of the putative neutral marker, *nuclear chloroplast-expressed Glutamine Synthetase* (*ncpGS*), showed that the *peloric* accessions are dispersed into multiple branches nested in wild gloxinias (supplementary fig. S11, Supplementary Material online). These results suggest that the *SsCYC* locus in *peloric* gloxinias was targeted by artificial selection, and the *peloric Sscyc* allele was derived from the sequence of "Cardoso Moreira" that is distinct from all other wild gloxinia accessions by a single domestication event.

Reconstructing the Domestication History of the *Peloric* Gloxinia

In the literature, the first *peloric* gloxinia with upright flowers was documented in 1845 under the name *Gloxinia fyfiana* (synonym of *S. speciosa*) produced by an Englishman called Fyfe by crossing *G. maxima* and *G. caulescens* in 1844 (both synonyms of *S. speciosa*) (fig. 8*A*) (Harrison 1847; Louis 1848; Fyfe 1879). *Gloxinia caulescens* was introduced from Brazil into England in 1820, published in 1827. It was widely cultivated and frequently crossed to *G. speciosa* due to its extravagant ornamental flowers (fig. 8*E*) (Edwards 1827; Paxton 1838; Maund and Henslow 1839; Harrison 1847; Johnson and Landreth 1847). *Gloxinia maxima* was recorded as a hybrid between *G. candida* and *G. speciosa* (both synonyms of *S. speciosa*) and published in 1838 (fig. 8*B*) (Paxton 1838). *Gloxinia speciosa* has horizontally orientated, zygomorphic flowers, and was introduced from Brazil into cultivation in England in 1815, published in 1817 (fig. 8*C*) (Loddiges 1817). *Gloxinia candida* first appeared in an exhibition in 1832 as a garden origin hybrid with no detailed character description except for white slipper flowers. The first "gloxinia" with white flowers, that is, *G. speciosa* var. *albiflora*, was published in 1833 (Hooker 1833). In 1839, another hybrid with white slipper flowers, similar to that of *G. candida*, was described in detail with a clear record that this hybrid was produced from a cross

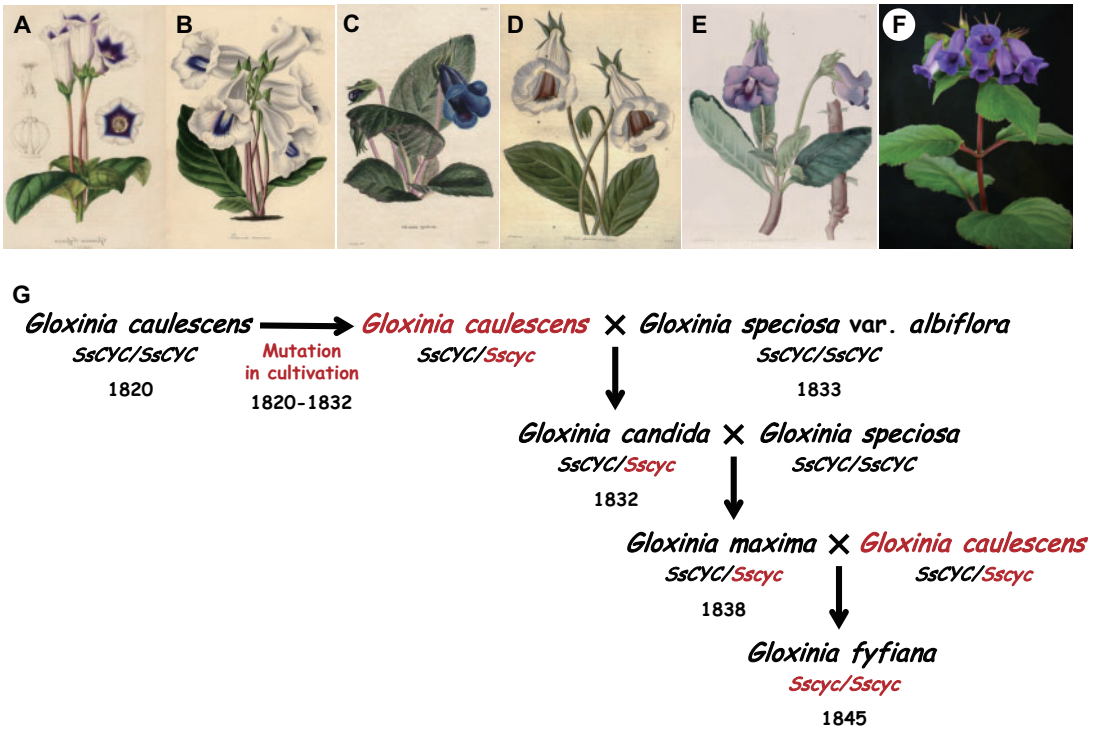

Fig. 8. Historical paintings of *Gloxinia* species and the genealogy of the first *peloric* gloxinia flower. (*A*) The original depiction of *G. fyfiana* in 1848 by Louis. (*B*) The original depiction of *G. maxima* in 1838 by Paxton. (*C*) The original depiction of *G. speciosa* in 1817 by Loddiges. (*D*) The original depiction of *G. speciosa-caulescens* hybrid in 1839 by Maund and Henslow. (*E*) The original depiction of *G. caulescens* in 1827 by Edwards. (*F*) Plant architecture of a flowering *S. speciosa* "Cardoso Moreira", showing the great morphological similarities to *G. fyfiana* (*A*) and *G. caulescens* (*E*) in terms of plant architecture. The photo is courtesy of Mr. Lin Ruei Chau. (*G*) The genealogy of the first *peloric* Gloxinia. The genotype and first appearance year of each "species" is indicated below, respectively. The *peloric* allele *Sscyc* and the mutated cultivar of *G. caulescens* are labeled in red. Note: the original imported *G. caulenscens* plants (1820) were supposed to be homozygous for *SsCYC*, as we failed to detect the mutated *Sscyc* allele in the wild populations. The *Sscyc* allele might have originated from the de novo mutation of 10-bp deletion in the cultivation process of *G. caulenscens* from 1820 to 1832 and kept a heterozygous (*SsCYC/Sscyc*) status in *G. candida* and *G. maxima* in the following 12 years before meeting with the mutated cultivar of *G. caulenscens* again in 1844. All the latin names presented in (*G*) are synonyms of *S. speciosa*.

between *G. speciosa* var. *albiflora* and *G. caulescens* (fig. 8*D*) (Maund and Henslow 1839). Since hybridization and breeding among "gloxinia" species was fashionable from 1820 to 1840 in Great Britain (Paxton 1838; Maund and Henslow 1839; Johnson 1847), it is possible that a hybrid with similar white slipper flowers was repeatedly produced from the crosses between *G. speciosa* var. *albiflora* and *G. caulescens* by gardeners at the time. Therefore, *G. candida* is probably a hybrid of *G. speciosa* var. *albiflora* × *G. caulescens*.

According to our results, the *peloric* allele is recessive and hence the *peloric* flower is homozygous for the *Sscyc* allele. In order to produce the *peloric* flower of *G. fyfiana*, both *G. maxima* and *G. caulescens* must possess a heterozygous *SsCYC/Sscyc* genotype. As for *G. maxima*, theoretically, it could have inherited the *peloric* allele from either *G. candida* or *G. speciosa*. As *G. speciosa* is a wild gloxinia introduced from Brazil, and because the probability of the same *peloric* mutation (10-bp deletion) happening independently in *G. caulescens* and *G. speciosa* is extremely low, we hypothesize that *G. speciosa* is unlikely to be the donor of the recessive *Sscyc* allele. It is more likely that *G. maxima* inherited the *peloric* allele from *G. candida* if we consider that the mutation occurred only once in *G. caulescens* specifically.

Taken together, the genetic inference above suggests that the causal mutation (10-bp deletion) leading to *peloric* gloxinia initially occurred in a cultivar of *G. caulescens* during the cultivation process between its importation in 1820 and the first appearance of the white-flowered hybrid (*G. candida*) in 1832 (fig. 8*G*). This mutation then passed from *G. candida* to *G. maxima* in 1838 and was kept in a heterozygous state for the following 6 years (1844) until *G. maxima* merging with the mutated heterozygous cultivar of *G. caulescens* in a cross generated by Mr. Fyfe (fig. 8*G*).

Discussion

On the Origin of the *Peloric* Gloxinia

The floral characteristics of ornamental plants have undergone an unprecedented explosion in color and morphology by deliberate hybridization-assisted selection over the past 200 years (Darwin 1868; Crane and Lawrence 1934; Kingsbury 2009). However, even for species whose domestication is clearly documented, showing major morphological transitions (e.g., Chinese primrose) (Crane and Lawrence 1934), the origin and spread of novel traits cannot be well understood until the genetic factors underlying these changes have been identified. Based on literature review and genetic

inferences, we propose that the causal mutation (10-bp deletion in *Sscyc*) leading to *peloria*, occurred only once, in a cultivar of *G. caulescens*. However, in the phylogenetic tree based on the ~1,250-bp of the *SsCYC* genomic sequence, the modern *peloric* gloxinias grouped together with two wild gloxinia collections from "Cardoso Moreira", suggesting that modern *peloric* gloxinia are derived from these two wild collections, or related populations. In fact, the wild "Cardoso Moreira" collections are closely related to the initial *peloric* gloxinia morphologically in plant architecture of extremely robust stems and one or two (or only several) flowers produced in the top leaf axils (fig. 8A, *E*, and *F*), suggesting that they are morphologically related. In addition, *G. caulescens* was originally recorded in wet rocks at the base of Corcovado Montain in Rio de Janeiro State in 1838 (Brackenridge 1886; Zaitlin 2011), adjacent to the location where the "Cardoso Moreira" samples were collected. Taken together, the genetic inferences and textual examination of the literature presented above strongly suggest that the "Cardoso Moreira" plants, or a related population of the same race, may be the gloxinia plants (designated as *G. caulescens*) exported from Brazil to Great Britain in 1820, which are the direct ancestors of the modern *peloric* gloxinia.

SsCYC Is a Pleiotropic Gene Controlling Multiple Floral Characters

Flowers are considered to be an essential model for studying the genetics of speciation, as the floral traits are intimately associated with prezygotic isolation (Smith 2016). Floral traits are often integrated as functional modules, which show correlated variation as the results of adaptation to specific pollination strategies (Fenster et al. 2009; Smith 2016). The genetic mechanism proposed to account for this complex morphological integration is that different characteristic elements are controlled by the same developmental gene with pleiotropic effects (Wagner and Zhang 2011; Smith 2016). In plants, genetic studies have identified a number of genomic regions responsible for multiple floral traits (Bradshaw et al. 1998; Wessinger et al. 2014). One caveat of these studies is that colocalization of multiple traits to the same genetic locus does not necessarily mean that the underlying genes or mutations are exactly the same, as a single locus may contain a large number of genes (Smith 2016). In addition, genes with pleiotropic effects identified in the functional analysis of model species are proposed to act as hot spots that facilitate phenotypic evolution (Wagner and Zhang 2011). However, direct molecular evidence for the evolution of functionally integrated phenotypic modules with the contribution of pleiotropic genes remain rare in plants, and the only examples are from animals (Linnen et al. 2013; Chung et al. 2014; Smith 2016). In *Sinningia speciosa*, our analysis provides three pieces of concrete evidence for the involvement of a pleiotropic gene in the development of an integrated floral character complex, that is, the nodding zygomorphic flower. Firstly, the anatomic examination shows that the nodding flower phenotype is caused by the development of a gibbous structure at the base of dorsal corolla. There is a simultaneous loss of the gibbous structure and zygomorphy in the *peloric* gloxinia, which lacks morphological recombination in the F_2 segregating population. This suggests that these characters are controlled by the same genetic regulator. Secondly, *SsCYC* exhibits dorsal specific expression in the floral organs (i.e., the dorsal petals and staminode) and inner parts of the basal dorsal floral tubes, which are correlated with the retardation of growth in the dorsal floral organs, and restricted cell expansion in the inner parts of the gibbous structure. Thirdly, the knockdown of *SsCYC* by dominant repression produces transgenic plants with perfectly ventralized actinomorphic flowers with loss of the gibbous structure, implying that the *SsCYC* is a pleiotropic gene responsible for the development of both morphological traits. The discovery of a *CYC*-like gene involved in the development of both floral symmetry and orientation provides empirical evidence that a simple genetic change in a pleiotropic gene with selective advantage would promote coordinated evolution of the highly integrated floral organs.

In angiosperms, the evolution of zygomorphic flowers is considered to be a major morphological innovation that led to the diversification of species (Dilcher 2000). It has been recently demonstrated that horizontal-orientated and zygomorphic flowers, with the two traits acting as a functional unit, confer a selective adaptive advantage, as they direct the pollinator movement within the flowers, and therefore, enable effective and precise pollen transfer to the stigma (Ushimaru and Hyodo 2005; Fenster et al. 2009; Wang et al. 2014). In fact, the association between the floral horizontal orientation and floral zygomorphy was recognized very early by Robertson in 1888. However, the floral orientation has long been neglected since then (Fenster et al. 2009). To our knowledge, this is the first time to report the role of *CYC*-like genes in controlling the floral orientation, expanding the function of *CYC*-like genes from controlling the floral symmetry to regulating both floral orientation and symmetry. This finding provides critical insights into how the high frequency of speciation with subsequent rapid diversification has occurred in zygomorphic lineages. In general, the floral horizontal orientation can be produced either by the asymmetrical growth of the floral tube or the bending of the pedicels relative to the stem. The floral zygomorphy coupled with floral horizontal orientation may have been independently evolved through different pathways. We also notice some cases of floral zygomorphy disassociated from horizontal orientation, such as some species of *Mimulus* (Phrymaceae) and *Agalinis* (Orobanchaceae) with zygomorphic but upright flowers. Further exploring the genetic basis relating to alternative pathways of the coupling between floral zygomorphy and horizontal orientation and the adaptive scenario for the decoupling between them in given taxa would shed new light on the mechanisms that underlie the vast morphological diversity of floral zygomorphy in angiosperms.

Materials and Methods

Plant Samples, Growth Condition and Artificial Hybridization

We chose Pink Flower (WT-PF) and White Bell (MU-WB) as plant materials for expression and functional analysis. WT-PF

is a wild-type gloxinia that is native to Brazil and produces large, horizontally oriented pink zygomorphic flowers with a white band decorated with dark purple spots in the ventral corolla throat. MU-WB is a popular cultivated variety widely cultivated in China, which bears upright white actinomorphic bell-shaped flowers. Various domesticated gloxinia accessions (supplementary table S2, Supplementary Material online) were either obtained from the Gesneriad Society (www.gesneriadsociety.org) or from commercial sources. The wild gloxinia (*S. speciosa*) collections and two *Sinningia* species (*S. tubiflora* and *S. rupicola*) were obtained as seed from Mauro Peixoto's Brazil Plants Organization (Mogi das Cruzes, SP, Brazil). The seeds were germinated on 1/2 Murashige and Skoog (MS) medium at 26 °C. The 1-month seedlings were then transplanted to 7-cm pots containing a mixture of moss substrate, vermiculite and perlite (1:1:1) in the glasshouse of Institute of Botany, the Chinese Academy of Sciences. Growth conditions were long-day photo period (16-h light/8-h dark) at 28 °C with a relative humidity of 70% and 60% shading.

Arabidopsis thaliana (ecotype Columbia-0) used in this study was germinated on 1/2 MS medium at 23 °C. The seedlings were transplanted in the soil under 16-h-light (200 μmol m^{-2} s^{-1}, 23 °C) and 8-h-dark (20 °C) conditions.

To generate the hybrid gloxinias, we pollinated the emasculated maternal plants (MU-WB) with pollen from the paternal plants (WT-PF) at anthesis. The resultant hybrids were germinated and transplanted into the glasshouse as described above.

Morphological Analysis and Scanning Electron Microscopy (SEM)

The floral organs of WT-PF and MU-WB at anthesis were dissected and the morphology of floral organs was recorded with Nikon D7100 camera.

For SEM, young inflorescences of WT-PF and MU-WB were fixed in FAA and infiltrated under vacuum. The respective floral meristems from distinct developmental stages were dissected with a needle in 70% ethanol under a light microscope. The materials were dried with critical point of CO_2 and the floral organs were examined using a Hitachi S-4800 scanning electron microscope (SEM) as previously described (Zhou et al. 2008).

To quantify cell size in the gibbous structure, the basal floral tube (including the gibbous structure) was fixed in FAA and embedded into paraffin (Sigma, USA). 8-μm sections were prepared using a rotary microtome. Section images were captured and processed by Image J (1.50b) software. For the gibbous structure, a total of 600 cells (12 cell layers, each layer five cells, ten sections) were examined for cell size variation, and a total of 500 cells (ten cell layers, each layer five cells, ten sections) were recorded in the ventral counterpart of the gibbous structure. Cell size was calculated according to the scale bars to generate the real size. Scatterplot analysis of cell size versus cell layer was conducted by Minitab17 (Minitab, Inc.), Gaussian Fitting (Curve Fitting Tool) was stimulated to show the variation tendency of cell size along the dorso-ventral axis of the gibbous structures and the ventral counterparts, respectively.

Genotyping and Association Analysis

The differences between *SsCYC* and *Sscyc* in the coding sequence allowed genotype specific CAPS primers to be designed (supplementary table S4, Supplementary Material online). A 624-bp fragment of *SsCYC* coding sequence was amplified by PCR and the purified products were subjected to *Nde*I digestion. For *Sscyc*, the 624-bp fragment is digested into 422 and 202-bp, whereas the *SsCYC* fragment cannot be digested and remains 624-bp after digestion. The segregation ratio and statistical analysis of the F_2 plants were performed using SPSS 14.0 software.

For SNP-phenotype association analysis, we isolated the 1922-bp 5′ promoter sequence by TAIL-PCR and sequenced 3,111-bp gDNA from a panel of 75 gloxinia accessions (supplementary table S2, Supplementary Material online). The initial sequences were aligned using Clustal X software (Thompson et al. 1997). The matrix was adjusted manually by using BioEdit Software (Hall 1999). Then, the matrix was imported into DnaSP 5.10 software (Librado and Rozas 2009) to generate the haplotype matrix by considering Indels as informative sites. The floral characters of 75 gloxinia accessions were recorded as *peloric* (1) and zygomorphic (0). The association of SNPs/Indels with phenotype was conducted by Tassel 5.0 software (Bradbury et al. 2007) under General Linear Model (GLM).

For annotation of the regulatory SNP in the promoters, we used online software TSSP (www.softberry.com) and PLACE (sogo.dna.affrc.go.jp) to predict the putative regulatory motifs in the 20-bp sequence including the significant associated SNPs.

RNA Extraction and Expression Analysis

Each floral organ was dissected and immediately frozen in liquid nitrogen. Total RNA was extracted using SV Total RNA Isolation System, and DNase I was added to digest the genomic DNA (Promega, USA) following the manufacturer's instructions. Complimentary DNA (cDNA) was synthesized using a RevertAid H Minus First-Strand cDNA Synthesis Kit (Thermo, USA) according to the manufacturer's instructions.

For real-time qPCR and allele specific gene expression of *SsCYCs*/*Sscyc*, we designed primers that specifically anchored to the 10-bp deletion difference between *SsCYC* and *Sscyc* (supplementary table S4, Supplementary Material online). Before conducting expression analysis, the specificity of the primers was verified by PCR and sequencing. The efficiency of the primers (95–105%) was determined by creating standard curve. The SYBR Premix ExTaq (TaKaRa, China) was used to perform real-time qPCR with ROX as a reference dye on a StepOne Plus Real-Time PCR System (Life Technology, USA). The CT value of each gene was determined by normalizing the fluorescence threshold. The relative expression level of the target gene was determined using the ratio $= 2^{-\Delta CT}$method, and *SsACT* was used as an internal control (Pfaffl 2001).

For RNA in situ hybridization, a 423-bp sequence targeted the 3′ coding sequence and 3′UTR of *SsCYC* was amplified

using primers (supplementary table S4, Supplementary Material online) designed to enhance the specificity and avoid cross-hybridization with other TCP genes. Digoxygenin-labeled probes were generated using an in vitro transcription system (Roche, Switzerland). RNA in situ hybridization experiments were conducted as previously described with minor modifications (Bradley et al. 1993). Briefly, young inflorescence and flowers of WT-PF and MU-WB were fixed in FAA and embedded in paraffin (Sigma, USA). 10-μm sections were prepared using a rotary microtome. After removing the paraffin, samples were hybridized with the antisense/sense probe of *SsCYC* at 42 °C for 16 h. Stringent formamide washings for nonspecific probes were performed after hybridization. The AP-conjugated anti-DIG antibodies (Roche, Switzerland) were then mounted on the samples for 2 h. After removing the nonspecific antibody, the samples were then incubated with the NBT/NCIP solution (Roche, Switzerland) for staining at room temperature for 10 h. The slides were dried and mounted with CC/mount medium (Sigma, USA). Samples were analyzed using the Zeiss Axio Imager A microscopy (Carl Zeiss, Germany).

Recombinant Protein Production and EMSA

A DNA fragment of 665-bp from the start codon of *SsCYC* or *Sscyc* was amplified from the WT-PF and MU-WB gDNA, respectively. The PCR product was digested with *BamH* I and *Hind* III and inserted into the pET30α vector (Merck, Germany). Constructed plasmids were verified by sequencing and then introduced into BL21 *Escherichia coli* cells. The His-tagged recombinant proteins were purified from the soluble fraction of the cell lysate using Ni sepharose (GE Healthcare, USA).

For EMSA, the 20 bp biotin-labeled probes were generated by Sangon Company (Sangon, Shanghai). EMSA was performed using nonradioactive NF-κB EMSA Kit (Thermo, USA) following the manufacturer's instructions. After the reaction, electrophoresis was conducted on a 6.5% nondenaturing polyacrylamide gel at 175 V in 0.25× TBE (22.25 mM Tris–HCl, 22.25 mM boric acid, and 5 mM EDTA, pH8.0) buffer at 4 °C for 1 h. The reaction products were transferred to the binding membrane at 394 mA in 0.5× TBE) at room temperature for 40 min. The probes were detected according to the manufacturer's instructions using the Imager Apparatus (Alpha, Canada). Two independent experiments were carried out to ensure that probe–protein interactions were specific.

Transgenic Analysis

For dominant repression of the SsCYC protein, the full length 1,035-bp *SsCYC*-CDS was fused in-frame with the EAR repression domain from the *SUPERMAN* gene and inserted downstream of the CaMV 35S promoter of the pCAMBIA 1301 vector to construct the SsCYC-SRDX vector. The vector was verified by sequencing and introduced into the *Agrobacterium tumefaciens* strain LBA4404 by electroporation. The transformation of *Sinningia speciosa* followed the methods described in Li et al. (2013) and Liu et al. (2014) with minor modifications (Li et al. 2013; Liu et al. 2014). Leaf discs from 8-weeks-old plantlets were precultured on MS medium containing 2 mg l^{-1} 2,4-dichlorophenoxy acetic acid (2,4-D) for 2 days. Discs were then subjected to infiltration with *Agrobacterium tumefaciens* (O.D. 600, 0.3) at room temperature for 15 min, transferred to the coculture MS medium containing 100 μM Acetosyringone (AS), and kept in the dark for 3 days. Resultant explants were transferred to selection MS medium containing 2 mg l^{-1} 6-Benzylaminopurine, 0.2 mg l^{-1} Naphthylacetic acid, 5 mg l^{-1} Hygromycin (Hyg) and 200 mg l^{-1} Cefotaxime (Cef). After six 2-week rounds of selection, regenerated Hyg-resistant adventitious shoots were obtained. The shoots were then transferred to MS medium for root induction. Discs of untransformed cultures were carried through the regeneration process as the wild type control. Transgenic and control plants were transplanted into the glasshouse as described above. For SsCYC-SRDX, a total of seven individual transgenic lines were obtained. The flower morphology of the transgenic plants was recorded with a Nikon D7100 camera.

For overexpression of *SsCYC*/*Sscyc* in *Arabidopsis*, the 1,267-bp of *SsCYC*/*Sscyc* g-DNA sequence encompassing the entire ORF was isolated from WT-PF and MU-WB, and inserted downstream of the CaMV 35S promoter of pCAMBIA 1301. Vectors were verified by sequencing and then introduced into *Agrobacterium tumefaciens* strain LBA4404 by electroporation. The resultant *Agrobacterium* was infiltrated into *Arabidopsis* using the floral dipping method (Clough and Bent 1998). Positive primary transformants were selected on 1/2 MS medium containing 40 mg/ml Hyg and 250 mg/ml Cef. Among the 45 SsCYC-OE T1 transformants, 39 showed a retarded plant development phenotype, with smaller rosette leaves and reproductive organs when compared with WT plants, whilst all 36 Sscyc-OE T1 transformants exhibited wild-type characteristics without any phenotypic changes. For each transgene, we randomly chose at least ten independent T1 transgenic plants, and selfed them to generated T_2 plants. The phenotypic analysis was performed on the T_2 population. To record leaf and petal parameters, the seventh leaf and sixth flower were collected for measurement by using a vernier. The SEM of leaf and petal epidermal cells was conducted as mentioned above.

Phylogenetic Analysis

We isolated the ~1,250-bp *SsCYC* from 23 wild gloxinia collections with WT phenotypes, 40 *peloric* gloxinias and two members of *Sinningia* (*S. tubiflora* and *S. rupicola*) which were used as an outgroup (supplementary table S2, Supplementary Material online). The sequences were aligned using Clustal X software and adjusted manually with the software Geneious version 7.1.4 (Kearse et al. 2012). Parsimony analysis was implemented in PAUP*4.0B10 (Swofford 2003). Bayesian inference analyses were carried out in MrBayes version 3.2.2 (Ronquist and Huelsenbeck 2003). Mrmodeltest version 2.3 (Nylander 2004) was used to select an appropriate model of sequence evolution for each DNA data set in Bayesian inference analyses. Bootstrap values of parsimony analysis and posterior probabilities (PP) obtained from the analysis were used to test the credibility of various branches. For the neutral marker *ncpGS*, we isolated a ~710-bp sequence from 20 wild

gloxinia collections, 19 *peloric* gloxinias, and two members of *Sinningia* (*S. tubiflora* and *S. rupicola*) which were used as outgroups (supplementary table S2, Supplementary Material online). The Phylogenetic analysis were conducted as aforementioned methods. For the phylogenetic analysis of *CYC*-like genes from Gesneriaceae species, the full-length protein sequences were downloaded from GenBank database and aligned with Clustal X software. The protein matrix was determined autoomatically in RAxML and 1000 bootstrap replicates were conducted in ML analysis. The Maximum likelihood (ML) tree with bootstrap support value was generated based on Protein sequence matrix by RAxML on the CIPRES Science Gateway Portal (Miller et al. 2010).

Population Genetic Analysis

We isolated the 3,111-bp gDNA sequence of *SsCYC* from 40 *peloric* gloxinia accessions from diverse locations around the globe and 23 wild gloxinia collections from Brazil (supplementary table S2, Supplementary Material online). Sequences were aligned by Clustal X software to generate the matrix (Thompson et al. 1997). Then the matrix was adjusted manually using BioEdit software and inputted into DnaSP 5.10 software (Hall 1999; Librado and Rozas 2009). Values of genetic diversity per base pair (π) were estimated for the domesticated *peloric* gloxinia and wild gloxinia groups. Sliding window analysis of genetic diversity was calculated using 100-bp window with a 25-bp step with average pairwise difference per base pair between sequences.

Supplementary Material

Supplementary data are available at *Molecular Biology and Evolution* online.

Acknowledgments

We thank André Kuhn, Feng-Xian Guo, Heather Bland, James F. Smith, Lukasz Langowski, Lars Østergaard, Pauline Stephenson, Rebecca Mosher, and three anonymous reviewers for their constructive comments. This study is funded by the National Natural Science Foundation of China (Grants 31470333, 31530003 to Yin-Zheng Wang and Grands 31400205 to Yang Dong) and the Financial Grant from the China Postdoctoral Science Foundation (Grants 2014M550878 and Grants 2015T80151 to Yang Dong).

Author's Contributions

Y.Z.W. initiated, conceived, designed, supervised the research and wrote the article. Y.D. conceived, designed and performed all the research, analyzed the data, and wrote the article. J.L. and P.W.L. were involved in the phylogenetic analysis. C.Q.L. and T.F.L. were involved in morphological and cellular analysis of the gibbous structure. X.Y. was involved in DNA sequence isolation. All authors read and approved the manuscript.

References

Amrad A, Moser M, Mandel T, de Vries M, Schuurink RC, Freitas L, Kuhlemeier C. 2016. Gain and loss of floral scent production through changes in structural genes during pollinator-mediated speciation. *Curr Biol*. 26(24):3303–3312.

Brackenridge WD. 1886. A chapter in the secret history of Gloxinia. *Gardeners' Monthly Horticulturist*. 28:59–60.

Bradbury PJ, Zhang Z, Kroon DE, Casstevens TM, Ramdoss Y, Buckler ES. 2007. TASSEL: software for association mapping of complex traits in diverse samples. *Bioinformatics* 23(19):2633–2635.

Bradley D, Carpenter R, Sommer H, Hartley N, Coen E. 1993. Complementary floral homeotic phenotypes result from opposite orientations of a transposon at the plena locus of *Antirrhinum*. *Cell* 72(1):85–95.

Bradshaw HD, Otto KG, Frewen BE, McKay JK, Schemske DW. 1998. Quantitative trait loci affecting differences in floral morphology between two species of monkeyflower (*Mimulus*). *Genetics* 149(1):367–382.

Chan YF, Marks ME, Jones FC, Villarreal G, Shapiro MD, Brady SD, Southwick AM, Absher DM, Grimwood J, Schmutz J. 2010. Adaptive evolution of pelvic reduction in sticklebacks by recurrent deletion of a *Pitx1* enhancer. *Science* 327(5963):302–305.

Chung H, Loehlin DW, Dufour HD, Vaccarro K, Millar JG, Carroll SB. 2014. A single gene affects both ecological divergence and mate choice in Drosophila. *Science* 343(6175):1148–1151.

Citerne HL, Möller M, Cronk QC. 2000. Diversity of cycloidea-like genes in Gesneriaceae in relation to floral symmetry. *Ann Bot*. 86(1):167–176.

Clough SJ, Bent AF. 1998. Floral dip: a simplified method for Agrobacterium-mediated transformation of *Arabidopsis thaliana*. *Plant J*. 16(6):735–743.

Crane MB, Lawrence WJC. 1934. The genetics of garden plants, 1st edn. London: Macmillan Press.

Cubas P, Coen E, Zapater JMM. 2001. Ancient asymmetries in the evolution of flowers. *Curr Biol*. 11(13):1050–1052.

Darwin C. 1865. The correspondence of Charles Darwin, Vol. 13. Cambridge: Cambridge University Press.

Darwin C. 1868. The variation of animals and plants under domestication, Vol. 1. London: The John Hopkins University Press.

Dilcher D. 2000. Toward a new synthesis: major evolutionary trends in the angiosperm fossil record. *Proc Natl Acad Sci U S A*. 97(13):7030–7036.

Doebley JF, Gaut BS, Smith BD. 2006. The molecular genetics of crop domestication. *Cell* 127(7):1309–1321.

Dong Y, Yang X, Liu J, Wang BH, Liu BL, Wang YZ. 2014. Pod shattering resistance associated with domestication is mediated by a NAC gene in soybean. *Nat Commun*. 5:3352.

Edwards S. 1827. *Gloxinia caulscens*. *Bot Reg*. 13:1127.

Fenster CB, Armbruster WS, Dudash MR. 2009. Specialization of flowers: is floral orientation an overlooked first step?. *New Phytol*. 183(3):502–506.

Fyfe J. 1879. Hints on the cultivation of choice gloxinias. *Gardeners' Month Horticulturist*. 21:359–362.

Gross BL, Olsen KM. 2010. Genetic perspectives on crop domestication. *Trends Plant Sci*. 15(9):529–537.

Hall TA. 1999. BioEdit: a user-friendly biological sequence alignment editor and analysis program for Windows 95/98/NT. *Nucleic Acids Symp Ser*. 41:95–98.

Harrison J. 1847. *Gloxinia fyfiana*. Mr Fyfe's Gloxinia. *Floricul Cabin*. 15:49–50.

Hileman LC. 2014. Bilateral flower symmetry-how, when and why?. *Curr Opin Plant Biol*. 17:146–152.

Hileman LC. 2014. Trends in flower symmetry evolution revealed through phylogenetic and developmental genetic advances. *Philos Trans R Soc B*. 369(1648):20130348.

Hiratsu K, Matsui K, Koyama T, Ohme-Takagi M. 2003. Dominant repression of target genes by chimeric repressors that include the EAR motif, a repression domain, in *Arabidopsis*. *Plant J*. 34(5):733–739.

Hoballah ME, Gubitz T, Stuurman J, Broger L, Barone M, Mandel T, Dell'Olivo A, Arnold M, Kuhlemeier C. 2007. Single gene-mediated shift in pollinator attraction in *Petunia*. *Plant Cell* 19(3):779–790.

Hooker WJ. 1833. *Gloxinia speciosa, var. albiflora*-showy gloxinia. *Curtis's Bot Mag*. 60:3206.

Hodges SA, Arnold ML. 1994. Floral and ecological isolation between *Aquilegia formosa* and *Aquilegia pubescens*. *Proc Natl Acad Sci U S A*. 91(7):2493–2496.
Hodges SA, Whittall JB, Fulton M, Yang JY. 2002. Genetics of floral traits influencing reproductive isolation between *Aquilegia formosa* and *Aquilegia pubescens*. *Am Nat*. 159 (S3):S51–S60.
Janick J. 2005. Horticultural plant breeding-past accomplishments, future directions. *Acta Hortic*. 694(694):61.
Johnson GW, Landreth D. 1847. A dictionary of modern gardening. Philadelphia: Lea and Blanchard Press.
Kearse M, Moir R, Wilson A, Stones-Havas S, Cheung M, Sturrock S, Buxton S, Cooper A, Markowitz S, Duran C, et al. 2012. Geneious basic: an integrated and extendable desktop software platform for the organization and analysis of sequence data. *Bioinfomatics* 28(12):1647–1649.
Kingsbury N. 2009. Hybrid: the history and science of plant breeding. Chicago: University of Chicago Press.
Linnen CR, Poh YP, Peterson BK, Barrett RD, Larson JG, Jensen JD, Hoekstra HE. 2013. Adaptive evolution of multiple traits through multiple mutations at a single gene. *Science* 339(6125):1312–1316.
Li C, Zhou A, Sang T. 2006. Rice domestication by reducing shattering. *Science* 311(5769):1936–1939.
Li X, Bian H, Song D, Ma S, Han N, Wang J, Zhu M. 2013. Flowering time control in ornamental gloxinia (*Sinningia speciosa*) by manipulation of miR159 expression. *Ann Bot*. 111(5):791–799.
Li J, Cocker JM, Wright J, Webster MA, McMullan M, Dyer S, Swarbreck D, Caccamo M, van Oosterhout C, Gilmartin PM. 2016. Genetic architecture and evolution of the *S* locus supergene in *Primula vulgaris*. *Nat Plants* 2(12):16188.
Librado P, Rozas J. 2009. DnaSP v5: a software for comprehensive analysis of DNA polymorphism data. *Bioinformatics* 25(11):1451–1452.
Liu BL, Pang HB, Yang X, Wang YZ. 2014. Functional and evolutionary analyses of *Primulina heterotricha CYC1C* gene in tobacco and *Arabidopsis* transformation systems. *J Syst Evol*. 52(1):112–123.
Liu BL, Yang X, Liu J, Dong Y, Wang YZ. 2014. Characterization, efficient transformation and regeneration of *Chirita pumila* (Gesneriaceae), a potential evo-devo model plant. *Plant Cell Tiss Organ Cult*. 118(2):357–372.
Loddiges C. 1817. *Gloxinia speciosa*. Rough-leaved Gloxinia. *Bot Mag*. 44:1937.
Louis VH. 1848. *Gloxinia fyfiana* (Hybrida). *Flore Des Serres Et Des Jardins De L'Europe* 4:311.
Luo D, Carpenter R, Copsey L, Vincent C, Clark J, Coen E. 1999. Control of organ asymmetry in flowers of *Antirrhinum*. *Cell* 99(4):367–376.
Luo D, Carpenter R, Vincent C, Copsey L, Coen E. 1996. Origin of floral asymmetry in *Antirrhinum*. *Nature* 383(6603):794–799.
Maund B, Henslow JS. 1839. Description of the hybrid, *Gloxinia speciosa-caulescens*. *Botanist* 3:149.
Miller MA, Pfeiffer W, Schwartz T. 2010. Creating the CIPRES Science Gateway for inference of large phylogenetic trees. Gatew. Comput. Enviro. Work, pp. 1–8.
Neal PR, Dafni A, Giurfa M. 1998. Floral symmetry and its role in plant-pollinator systems: terminology, distribution, and hypotheses. *Annu Rev Ecol Syst*. 29(1):345–373.
Nylander JAA. 2004. MrModeltest Version 2. Program distributed by the author. (Uppsala University, Uppsala, Sweden). Available at http://people.scs.fsu.edu/nylander/mrmodeltest2/mrmodeltest2.html.
Paxton J. 1838. *Gloxinia maxima*. *Paxton's Mag Bot Reg*. 5:219–220.
Paxton J. 1838. *Gloxinia speciosa* and caulescens. *Paxton's Mag Bot Reg*. 4:127.
Pfaffl MW. 2001. A new mathematical model for relative quantification in real-time RT-PCR. *Nucleic Acids Res*. 29(9):e45.
Pourkheirandish M, Hensel G, Kilian B, Senthil N, Chen G, Sameri M, Azhaguvel P, Sakuma S, Dhanagond S, Sharma R, et al. 2015. Evolution of the grain dispersal system in barley. *Cell* 162(3):527–539.
Preston JC, Hileman LC. 2009. Developmental genetics of floral symmetry evolution. *Trend Plant Sci*. 14(3):147–157.
Rieseberg LH, Blackman BK. 2010. Speciation genes in plant. *Ann Bot*. 106(3):439–455.
Robertson C. 1888. Zygomorphy and its causes I–III. *Bot Gaz*. 13:146–151. 203-208, 224-230.
Ronquist F, Huelsenbeck JP. 2003. MrBayes 3: Bayesian phylogenetic inference under mixed models. *Bioinformatics* 19(12):1572–1574.
Sheehan H, Moser M, Klahre U, Esfeld K, Dell'Olivo A, Mandel T, Metzger S, Vandenbussche M, Freitas L, Kuhlemeier C. 2016. MYB-FL controls gain and loss of floral UV absorbance, a key trait affecting pollinator preference and reproductive isolation. *Nat Genet*. 48(2):159.
Smith JF, Hileman LC, Powell MP, Baum DA. 2004. Evolution of *GCYC*, a Gesneriaceae homolog of *CYCLOIDEA*, within Gesnerioideae (Gesneriaceae). *Mol Phyl Evol*. 31(2):765–779.
Smith SD. 2016. Pleiotropy and the evolution of floral integration. *New Phytol*. 209(1):80–85.
Song CF, Lin QB, Liang RH, Wang YZ. 2009. Expressions of ECE-CYC2 clade genes relating to abortion of both dorsal and ventral stamens in *Opithandra* (Gesneriaceae). *BMC Evol Biol*. 9(1):244.
Specht CD, Bartlett ME. 2009. Flower evolution: the origin and subsequent diversification of the angiosperm flower. *Annu Rev Ecol Syst*. 40(1):217–243.
Sprengel CK. 1793. Das Entdeckte Geheimniss in der Natur im Bau und in der Befuchtung der Blumen. Berlin: Friedrich Vieweg Press.
Studer A, Zhao Q, Ross-Ibarra J, Doebley J. 2011. Identification of a functional transposon insertion in the maize domestication gene *tb1*. *Nat Genet*. 43(11):1160–1163.
Swofford DL. 2003. PAUP*. Phylogenetic analysis using parsimony (* and other methods). Version 4. Sunderland MA: Sinauer Associates.
Thompson JD, Gibson TJ, Plewniak F, Jeanmougin F, Higgins DG. 1997. The CLUSTAL_X windows interface flexible strategies for multiple sequence alignment aided by quality analysis tools. *Nucleic Acids Res*. 25(24):4876–4882.
Ushimaru A, Hyodo F. 2005. Why do bilaterally symmetrical flowers orient vertically? Flower orientation influences pollinator landing behaviour. *Evol Ecol Res*. 7(1):151–160.
Wagner GP, Zhang JZ. 2011. The pleiotropic structure of the genotype–phenotype map: the evolvability of complex organisms. *Nat Rev Genet*. 12(3):204–213.
Wang H, Tie S, Yu D, Guo YH, Yang CF. 2014. Change of floral orientation within an inflorescence affects pollinator behavior and pollination efficiency in a bee-pollinated plant, *Corydalis sheareri*. *PloS One* 9(4):e95381.
Wessinger CA, Hileman LC, Rausher MD. 2014. Identification of major quantitative trait loci underlying floral pollination syndrome divergence in *Penstemon*. *Philos Trans R Soc B*. 369(1648): 20130349.
Yang X, Pang HB, Liu BL, Qiu ZJ, Gao Q, Wei L, Dong Y, Wang YZ. 2012. Evolution of double positive autoregulatory feedback loops in *CYCLOIDEA2* clade genes is associated with the origin of floral zygomorphy. *Plant Cell* 24(5):1834–1847.
Yang X, Zhao XG, Li CQ, Liu J, Qiu ZJ, Dong Y, Wang YZ. 2015. Distinct regulatory changes underlying differential expression of teosinte branched1-cycloidea-proliferating cell factor genes associated with petal variations in zygomorphic flowers of *Petrocosmea spp*. of the family Gesneriaceae. *Plant Physiol*. 169(3):2138–2151.
Zaitlin D. 2011. A history of the florist gloxinia in pictures and words. *Gesneriad* 3:14–27.